Comparing Molecular Packing and Textures of Langmuir Monolayers of Fatty Acids and Their Methyl and Ethyl Esters

G. Weidemann, G. Brezesinski, D. Vollhardt,* F. Bringezu, K. de Meijere, and H. Möhwald

Max-Planck-Institut für Kolloid- und Grenzflächenforschung, Rudower Chaussee 5, 12489 Berlin, Germany

Received: June 20, 1997; In Final Form: September 9, 1997[⊗]

Langmuir monolayers of fatty acids and their methyl and ethyl esters show different textures. Stripe textures are observed in myristic acid monolayers. Continuous changes of molecular orientation occur in palmitic acid layers as well, although there are no stripe textures. In monolayers of fatty acid methyl and ethyl esters such continuous changes of orientation are not observed. The domains of methyl palmitate and ethyl palmitate are subdivided into segments of equal brightness. Grazing incidence synchrotron X-ray diffraction (GID) studies were performed to analyze the reason for this deviating behavior at the molecular level. The diffraction patterns of myristic acid suggest that the tilt azimuth is dispersed by about 5° around a nearest-neighbor direction. Such dispersions of the tilt azimuth occur in palmitic acid and methyl palmitate layers as well. The monolayers of these substances differ from those of myristic acid only in the degree of the dispersion.

Introduction

Lipid monolayers are suitable model systems for studying a variety of questions in physics chemistry and biology. One of these is to relate lattice structure and morphology, an important question in materials science. Owing to the two-dimensional nature of the film, the growth process occurs exclusively parallel to the plane. Textures of domains can be quantified by optical techniques, and there are now also techniques to study the lattice structure.

The phase diagram of fatty acid monolayers at the air/water interface has been widely studied, both with optical microscopy[1] and grazing incidence X-ray diffraction (GID).[2−5] In addition to fatty acids, methyl and ethyl esters of fatty acids have also been studied.[6,7] Although GID has been used for studies of fatty acids with at least 18 carbon atoms, Brewster angle microscopy (BAM) and polarized fluorescence microscopy have been used for the characterization of shorter molecules.[7−15] Phase transitions with a change of the tilt azimuth with respect to the lattice directions can be studied easily by BAM, since they cause macroscopic reorientation in the monolayers.[1,6,7]

The characterization of the layers with microscopy uses the long-range tilt orientational order in the monolayers to draw conclusions about monolayer phases.[7−15] From the stripe textures in monolayers of myristic acid and pentadecanoic acid it was inferred that the monolayer phase is comparable to smectic I.[11b,20,21] Fatty acid methyl esters do not show such stripes.[13,15] The domains are subdivided into six regions of homogeneous orientation, a texture that resembles the star textural defect in thin smectic liquid crystal layers.[16] In fatty acid ethyl ester monolayers, again domains with a 6-fold subdivision are observed.[10] The orientation of the molecules with respect to the domain boundary is, however, different. Whereas the tilt azimuth is preferentially perpendicular to the boundary in methyl palmitate layers[15] a preferred tilt azimuth parallel to the boundary is found in ethyl palmitate layers.[10]

The most direct way to learn about the nature of the phases of a monolayer is based on grazing incidence diffraction. By use of the setup at BW1, HASYLAB, it is possible to get diffraction data of good quality from monolayers of substances with C_{15} and even C_{13} chains. In the present paper monolayers of myristic acid, palmitic acid, methyl palmitate, and ethyl palmitate are studied. Owing to this material selection, we could study the influence of the headgroup structure on the textures and on the structure of the condensed phases. Furthermore, the reason for the different textures in these layers can be analyzed.

Experimental Section

Materials. The subphase water used for the experiments was purified by a Millipore desktop (Millipore, Eschborn). Myristic acid, palmitic acid, methyl palmitate and ethyl palmitate were purchased from Sigma, Deisenhofen (approximately 99% pure) and used without further purification. The heptane that is used for spreading was obtained from Merck, Darmstadt (UVASOL). For the studies of fatty acid monolayers the pH of the subphase water was adjusted to 2 with HCl (Titrisol) from Merck, Darmstadt.

Brewster Angle Microscopy. Monolayers were observed with a Brewster angle microscope (BAM1 from NFT, Göttingen) mounted on a Langmuir film balance from Lauda (FW2). The BAM images presented here are mirror images of the monolayer, since, in the BAM1, the reflected beam is directed by a mirror into the CCD camera. BAM images are distorted owing to the observation at the Brewster angle. An image-processing software was used to correct the digitized images for the distortion. The lateral resolution of the BAM1 is about 4 μm. Since only a small part of the image is sufficiently sharp and well illuminated, the figures in the present work are parts (500 μm × 500 μm) of the original images.

Grazing Incidence Diffraction. Grazing incidence X-ray diffraction experiments were performed using the liquid−surface diffractometer on the undulator beam-line BW1 at HASYLAB, DESY, Hamburg, Germany. The beam was made monochromatic by a beryllium crystal (002). The wavelength was 1.481 Å (except for the ethyl palmitate study, where it was 1.324 Å).

[⊗] Abstract published in *Advance ACS Abstracts,* December 15, 1997.

S1089-5647(97)02025-7 CCC: $15.00
Published on Web 01/01/1998

The beam was adjusted to strike the surface with angle of incidence $\alpha_i \approx 0.85\alpha_c$, where α_c ($\alpha_c \approx 0.14°$) is the critical angle for total internal reflection. The diffracted intensity was monitored by a linear position sensitive detector (PSD) (OED-100-M, Braun Garching, Germany). The in-plane divergence of the diffracted beam was restricted to 0.09° by a Soller collimator in front of the PSD. According to the geometry of diffraction,[17] the scattering vector **Q** can be written in terms of an in-plane component Q_{xy} with

$$Q_{xy} = \frac{2\pi}{\lambda}\sqrt{\cos^2 \alpha_i + \cos^2 \alpha_f - 2 \cos \alpha_i \cos \alpha_f \cos 2\theta} \quad (1)$$

and an out-of plane component Q_z with

$$Q_z = \frac{2\pi}{\lambda}(\sin \alpha_i + \sin \alpha_f) \quad (2)$$

where α_f and 2θ are the vertical and the horizontal scattering angle, respectively.

The intensities were least-squares fitted as a Lorentzian parallel to the water surface and as a Gaussian normal to it. From the in-plane peak positions the lattice spacings can be obtained.

$$Q_{xy} = \frac{2\pi}{d_{hk}} \quad (3)$$

The full width at half-maximum fwhm is related to the positional correlation length ξ. For an exponential decay of positional correlation as observed in liquid crystals (corresponding to a Lorentzian peak profile), it is

$$\xi = \frac{2}{\text{fwhm}(Q_{xy})} \quad (4)$$

The out-of-plane scattering component can provide information about the polar tilt angle Ψ and the tilt azimuth of the alkyl chains. According to the cylinder model,[17] the scattering vector components at the position of the maximum are related to these two parameters:

$$Q_z^{hk} = Q_{xy}^{hk} \cos \Psi_{hk} \tan t \quad (5)$$

For a rectangular lattice two peaks are observed: the (02) and the degenerate (11), ($1\bar{1}$) peaks. Deviations from a rectangular lattice repeal this degeneration, and the peaks shift in opposite directions.

The fwhm of the Gaussian profile of the peak normal to the surface is given by the length L of the molecules:

$$\text{fwhm}(Q_z) = \frac{0.9 \cdot 2\pi}{L} \quad (6)$$

Consequently, the peaks of a substance are expected to have the same fwhm normal to the surface.

Results

Myristic acid monolayers were studied at 10 °C. Regular stripes are observed with a width depending on the surface pressure. At 15 mN/m the stripes are about 50 μm wide (Figure 1a); however, the contrast is quite poor. A decrease of surface pressure leads to an increase of chain tilt and thus to an increase of anisotropy contrast. The width of the stripes decreases with surface pressure to about 15 μm at 10 mN/m (Figure 1b) and below 10 μm at 5 mN/m (Figure 1c), in agreement with the literature.[11a] In monolayers of palmitic acid at 24 °C, large areas are covered with condensed material (Figure 1d, right part). Additionally, some domains (Figure 1d, left) that are quite similar to the shell textures known for pentadecanoic acid[12a] can be observed. Regular stripes do not occur.

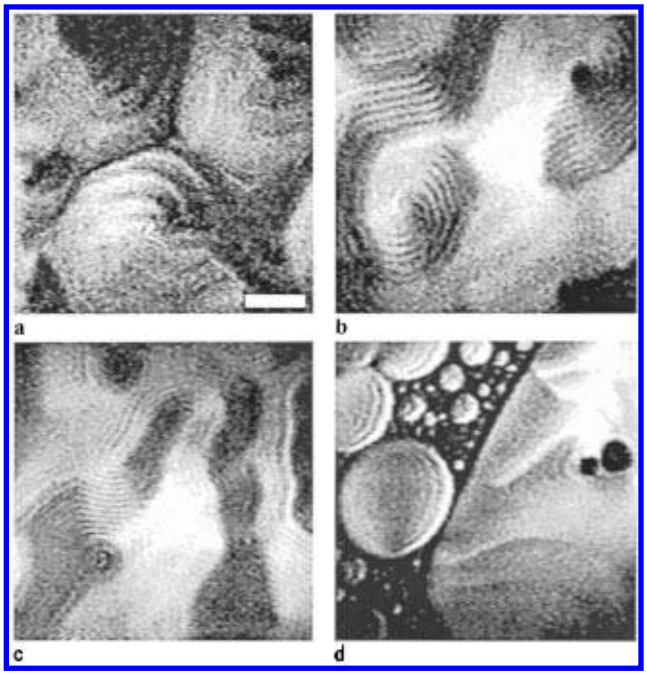

Figure 1. At 10 °C the condensed phase in myristic acid monolayers is formed in a first-order phase transition from a fluid phase ($\pi \approx 4$ mN/m). Regular stripes are formed if the monolayer is first compressed to a state with vertical chains and subsequently expanded. Monolayer is shown at 15 mN/m (a), 10 mN/m (b), and 5 mN/m (c). In palmitic acid monolayers the condensed phase is formed during spreading at 24 °C (d). The bar represents 100 μm.

In methyl palmitate monolayers, the domains of the condensed phase are subdivided into six segments of different brightness (Figure 2a). Within these segments, changes of orientation were not observed. The tilt azimuth of the alkyl chains runs along the bisector of these segments[15] (Figure 2b). The domains in ethyl palmitate monolayers are also subdivided into six segments at 16 °C (parts c and d of Figure 2), but the alkyl chains are now tilted perpendicular and not parallel to the bisector of the segments[10] (parts e and f of Figure 2). Thus, domains with clockwise and counterclockwise changes of orientation can be observed. These domains differ with respect to the positions of segments with equal reflectivity. At 20 °C the same domain morphology is observed, only the contrast is reduced owing to the decreased polar tilt angle of alkyl chains.

With GID, two peaks corresponding to a centered rectangular lattice are observed for myristic acid monolayers at 10 °C (Figure 3). The peak positions are given in Table 1. At 5 mN/m the chains are tilted by 27° toward nearest neighbors (Table 2). The polar tilt angle decreases to 18° at 15 mN/m and to 9° at 20 mN/m. The peak with the high Q_z value, which was identified as the degenerate (11), ($1\bar{1}$) peak, is asymmetric. The maximum position in the *xy* direction shifts with Q_z (see Table 3). The isotherms show that the chains become upright at about 22 mN/m, coinciding with the vanishing anisotropy contrast in the BAM. Palmitic acid layers show a rectangular lattice with chains tilted by 25° toward nearest neighbors (NN) at 10 mN/m (Figure 4a) and tilted by 16° toward next-nearest neighbors (NNN) at 18 mN/m (Figure 4b). At 25 mN/m a hexagonal lattice of vertical chains is observed. The chains again become upright at about 22 mN/m (Figure 4c).

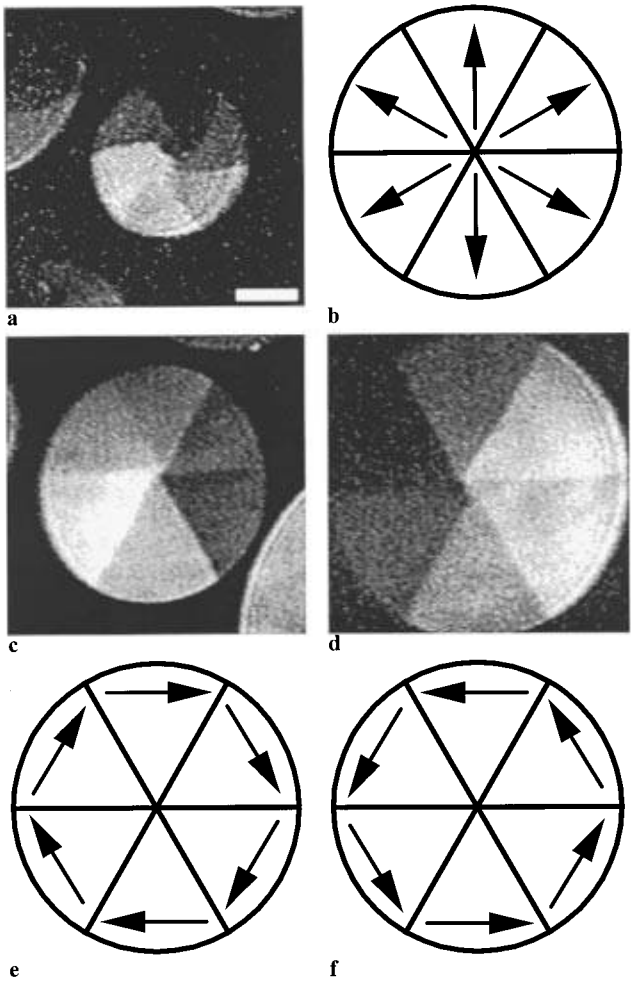

Figure 2. In methyl palmitate monolayers at 25 °C the domains of condensed phase are formed in a phase coexistence region from a fluid phase ($\pi \approx 4$ mN/m) (a). Sketch of the orientation in the domain is shown in (b). Two types of domains are formed in ethyl palmitate layers (c, d) from the fluid phase at 16 °C ($\pi \approx 2$ mN/m). In one type the tilt azimuth changes clockwise (e); in the other it changes counterclockwise (f). The bar represents 100 μm.

For the methyl and ethyl esters the chains are less tilted than for the fatty acids (Table 2). Consequently, the peaks start to overlap (Figures 5 and 6). In methyl palmitate layers the diffracted intensity of the peak with the higher Q_z value was very low at 1 mN/m. Thus, it was not possible to determine its position very accurately. The polar tilt angle is about 17°, the chains are NN-tilted. At 7 mN/m the polar tilt angle is reduced to 9°, the chains remain NN-tilted (Figure 5a). At 14 mN/m the chains stand upright (Figure 5b). BAM studies reveal that the chains become upright at about 10 mN/m and that no transition between tilted monolayer phases occurs. Such a transition was also ruled out for ethyl palmitate monolayers by BAM measurements. The transition to vertical chains is at 9 mN/m at 16 °C and at 8 mN/m at 20 °C. For both temperatures the diffracted intensity is shown at 14 mN/m in parts b and d of Figure 6. Two overlapping peaks occur at 4 mN/m and 16 °C as well as at 6 mN/m and 20 °C (parts a and c of Figure 6). The peaks were quite noisy at 16 °C, since the diffracted intensity was low (Figure 6a). The peaks are perceptibly separated at 20 °C. The overlap of the peaks impedes an analysis of the Q_z positions. However, taking into consideration that the fwhm(Q_z) should have about the same value for all peaks (since the fwhm(Q_z) is only correlated to the length of the molecule), one is forced to conclude that the chains are NNN-

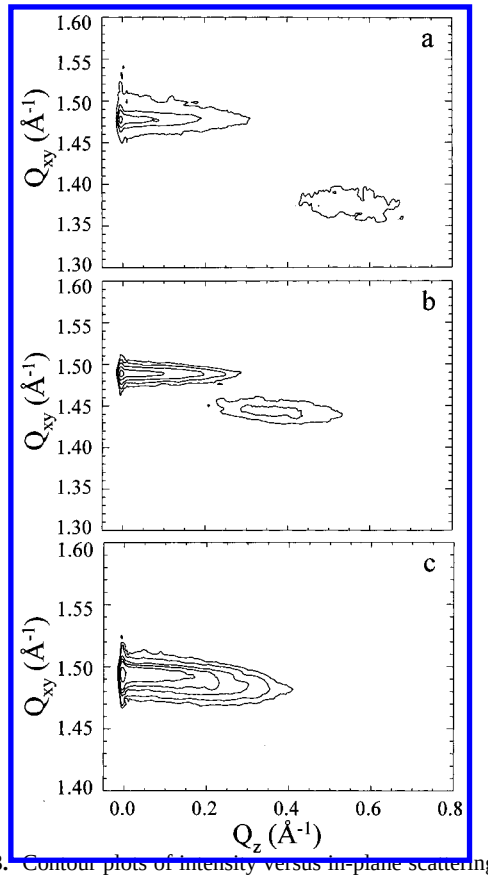

Figure 3. Contour plots of intensity versus in-plane scattering vector component Q_{xy} and out-of-plane scattering vector component Q_z for myristic acid at 10 °C and 5 mN/m (a), 15 mN/m (b), and 20 mN/m (c).

TABLE 1: Peak Positions (Printed Bold) and fwhm (below the Peak Positions)

substance, conditions	π [mN/m]	(02) Q_{xy} [Å^{-1}]	(02) Q_z [Å^{-1}]	(11), (1$\bar{1}$) Q_{xy} [Å^{-1}]	(11), (1$\bar{1}$) Q_z [Å^{-1}]
myristic acid, pH 2, 10 °C	5	**1.478**	0	**1.376**	**0.60**
		0.018		0.039	0.54
	15	**1.489**	0	**1.443**	**0.40**
		0.016		0.030	0.32
	20	**1.493**	0	**1.483**	**0.20**
		0.017		0.016	0.32
palmitic acid, pH 2, 24 °C	10	**1.483**	0	**1.406**	**0.55**
		0.013		0.036	0.29
	18	**1.446**	**0.42**	**1.480**	**0.21**
		0.022	0.29	0.026	0.29
	25	**1.502**	0		
		0.010			
methyl palmitate, 22 °C	1	**1.510**	0	∼**1.46**[a]	**0.4**
		0.017		*a*	*a*
	7	**1.514**	0	**1.498**	**0.20**
		0.011		0.022	0.27
	14	**1.517**	0		
		0.012			
	20	**1.520**	0		
		0.011			
ethyl palmitate, 16 °C	4	**1.480**	**0.34**	**1.507**	**0.17**
		∼0.04[a]	0.26	∼0.02[a]	0.31
	14	**1.517**	0		
		0.016			
ethyl palmitate, 20 °C	6	**1.496**	**0.23**	**1.508**	**0.11**
		∼0.02[a]	0.25	∼0.02[a]	0.30
	14	**1.513**	0		
		0.018			

[a] For methyl palmitate the low intensity does not allow a determination at all or a precise determination, whereas for ethyl palmitate the lower precision is caused by the overlap of peaks.

TABLE 2: Lattice Parameters

	a [Å]	b [Å]	A_{xy} [Å^2]	t [deg]	TA	A_o [Å^2]
myristic acid, pH 2, 10 °C						
5 mN/m	5.413	8.502	23.0	27	NN	20.4
15 mN/m	5.083	8.439	21.4	18	NN	20.4
20 mN/m	4.903	8.417	20.6	9	NN	20.4
palmitic acid, pH 2, 24 °C						
10 mN/m	5.259	8.474	22.3	25	NN	20.2
18 mN/m	4.865	8.690	21.1	16	NNN	20.3
25 mN/m	4.830	8.366	20.2	0		20.2
methyl palmitate, 22 °C						
1 mN/m[a]	5.028	8.322	20.9	17	NN	20.0
7 mN/m	4.861	8.300	20.2	9	NN	19.9
14 mN/m	4.782	8.284	19.8	0		19.8
20 mN/m	4.773	8.267	19.7	0		19.7
ethyl palmitate, 16 °C						
4 mN/m	4.786	8.491	20.3	13	NNN	19.8
14 mN/m	4.783	8.284	19.8	0		19.8
ethyl palmitate, 20 °C						
6 mN/m	4.798	8.400	20.2	9	NNN	19.9
14 mN/m	4.795	8.306	19.9	0		19.9

[a] Values not very precise because of low diffraction intensity.

TABLE 3: Shift of the Q_{xy} Peak Position from High to Low Q_z Values

		Q_{xy} [Å^{-1}] (11), (1$\bar{1}$)	
substance, conditions	π [mN/m]	$Q_z\downarrow$	$Q_z\uparrow$
myristic acid, pH 2, 10 °C	5	1.386	1.368
	15	1.448	1.434
palmitic acid, pH 2, 24 °C	10	1.409	1.403
	18	1.483	1.478
methyl palmitate, 22 °C	7	1.500	1.496

tilted with $t \approx 13°$ at 16 °C and 4 mN/m and $t \approx 9°$ at 20 °C and 6 mN/m (Table 2). This interpretation is also supported by the intensities of the peaks. The degenerate (11), (1$\bar{1}$) peak is expected to have about twice the intensity of the (02) peak. This agrees with the lower intensity of the peak with the higher Q_z value, which is the (02) peak for NNN tilt (parts a and c of Figure 6).

Discussion

The textures in the monolayers of fatty acids deviate drastically from those in the monolayers of the fatty acid methyl and ethyl esters. At first glance, the lattices of all these monolayers are rectangular if the chains are tilted. For myristic and palmitic acid as well as for methyl palmitate the chains are NN-tilted. Only in ethyl palmitate layers does the tilt azimuth run along an NNN direction. In all monolayers studied here the cross-sectional area of alkyl chains is about 20 Å^2 as in free rotator phases of *n*-alkanes. The highest values are observed for myristic acid and the lowest values for the methyl and ethyl esters (Table 2). A comparison of myristic and palmitic acid shows that the cross-sectional area decreases with increasing alkyl chain length.

The striking difference between fatty acids and their methyl and ethyl esters is the magnitude of the tilt of the alkyl chains. For a comparison of the polar tilt angles, it is convenient to extrapolate them to zero surface pressure, assuming that the area per molecule decreases linearly with surface pressure. Then $1/\cos(t)$ also decreases linearly with surface pressure. The t values at zero pressure obtained by this procedure are 33° for palmitic acid, 30° for myristic acid, 18° for methyl palmitate, and 16° for ethyl palmitate. This order is opposite to what one would have expected, since the hydrophobic methyl and ethyl groups might fold back into the hydrophobic region and thus increase the tilt angle. This is obviously not the case, and the untilted tail arrangement can be achieved with methylated and even ethylated headgroups.

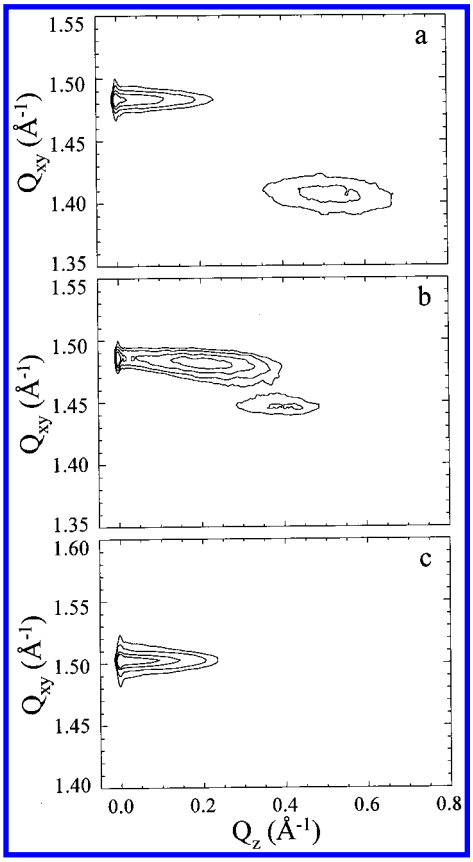

Figure 4. Contour plots of intensity versus in-plane scattering vector component Q_{xy} and out-of-plane scattering vector component Q_z for palmitic acid at 24 °C and 10 mN/m (a), 18 mN/m (b), and 25 mN/m (c).

A comparison of the substances with respect to the positional correlation length ξ for the state with upright chains gives $\xi >$ 200 Å for palmitic acid at 25 mN/m (fwhm(Q_{xy}) is resolution limited). The methyl ester has a decreased positional correlation length of 180 Å at 20 mN/m. For ethyl palmitate ξ amounts only to 150 Å at 16 °C and 14 mN/m. Consequently, the positional correlation length decreases from palmitic acid to methyl palmitate and ethyl palmitate. For all monolayers a

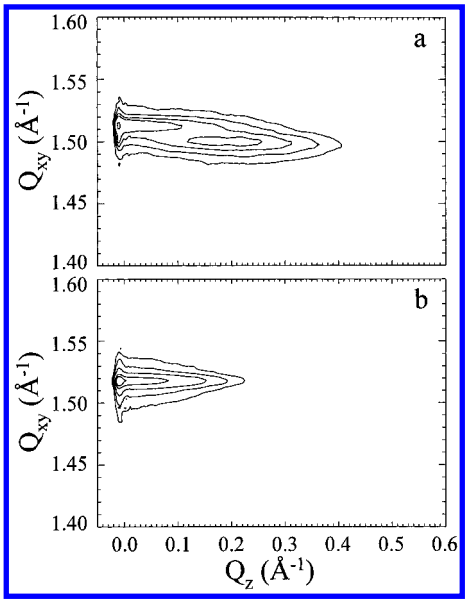

Figure 5. Contour plots of intensity versus in-plane scattering vector component Q_{xy} and out-of-plane scattering vector component Q_z for methyl palmitate at 22 °C and 7 mN/m (a) and 14 mN/m (b).

decrease of ξ with decreasing surface pressure is observed but ξ does not fall below 100 Å for the nondegenerate (02) peak.

What is the reason for the different textures in the monolayers? For ethyl palmitate NNN-tilted chains with a small polar tilt angle are characteristic, whereas the chains are NN-tilted for methyl palmitate. This explains the differences in the textures of methyl and ethyl palmitate layers. A tilt azimuth aligned parallel to the domain boundary seems to be typical for phases with NNN tilt.[10] From BAM studies it becomes evident that in the temperature range from 8 to 24 °C no phase transition between tilted monolayer phases occurs. Fatty acids differ from its methyl and ethyl esters by the higher polar tilt angle. The stripe textures in myristic acid layers cannot, however, be explained by the higher tilt angle of fatty acids. Similar high-tilt angles have been found for other substances such as 1-monopalmitin for which no continuous changes of orientation are observed in the monolayers.[8] A perceptible difference in the diffraction pattern is the asymmetric (11), ($1\bar{1}$) peak in myristic acid monolayers. The continuous shift of the Q_{xy} value of the peak maximum with Q_z cannot be explained by the superposition of only two peaks slightly shifted, which would arise if the tilt azimuth deviates from 0°. Furthermore, the maximum of the (02) peak remains at $Q_z = 0$ Å^{-1}. In the z direction the fwhm(Q_z) of the peak is, however, about 0.54 Å^{-1} (at the maximum with respect to Q_{xy}). This is much more than the approximately 0.3 Å^{-1} that one expects from the length of the molecule of about 20 Å. The continuous shift of the Q_{xy} values with increasing Q_z over the whole Q_z range of the peak gives rise to the assumption that the tilt azimuth has no fixed value but rather is dispersed around 0°. The extent of the shift correlates then with the extent of the dispersion of the tilt azimuth.

A rough estimate of the dispersion range of the tilt azimuth requires a calculation of the lattice as a function of the tilt azimuth. The in-plane lattice and the lattice in the plane perpendicular to the alkyl chain axis (i.e., the chain packing) are related to each other. The in-plane lattice is elongated with respect to the chain packing by a factor of $1/\cos(t)$ in tilt direction. Assuming a constant cross-sectional area of chains, a constant polar tilt angle, and hexagonal packing of chains perpendicular to their axis, the in-plane lattice and thus the peak

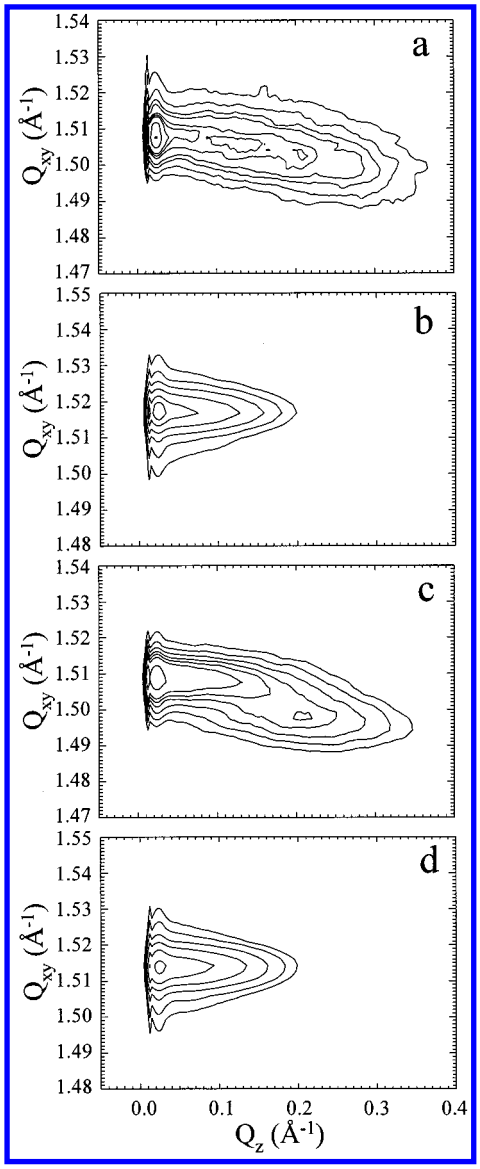

Figure 6. Contour plots of intensity versus in-plane scattering vector component Q_{xy} and out-of-plane scattering vector component Q_z for ethyl palmitate at 16 °C and 4 mN/m (a) and 14 mN/m (b) and at 22 °C and 6 mN/m (c) and 14 mN/m (d).

positions can be calculated as a function of the tilt azimuth.[18] A deviation of the tilt azimuth from 0° results in a separation of the (11) and ($1\bar{1}$) peak. Both peaks shift in opposite directions both in Q_{xy} and Q_z. The shift of the peak position observed for myristic acid (Table 3) corresponds to a dispersion of the tilt angle by about 5°. The decrease of the shift with surface pressure is caused by the decrease of the polar tilt angle but not by a reduced dispersion of the tilt azimuth. Consequently, the extent of the dispersion of the tilt azimuth does not correlate with the width of the stripes in myristic acid layers.

The fwhm(Q_{xy}) of the (11), ($1\bar{1}$) peak is found to be larger than that of the (02) peak. This seems to be caused by the superposition of the peaks from lattices with different chain tilt azimuths. The positional correlation length calculated from the (02) peak is about 120 Å. However, another contribution to the increased fwhm(Q_{xy}) of the (11), ($1\bar{1}$) peak exists if the chains are NN-tilted. Deviations of the water surface from the horizontal, which might be introduced by waves or the meniscus, give rise to an increase of fwhm(Q_{xy}) with increasing Q_z as well.[19] This might explain the result for palmitic acid at 18 mN/m. There the chains are NNN-tilted and the fwhm(Q_{xy}) of

the (02) peak, which now has the higher Q_z value, is increased. Furthermore, different positional correlation lengths along different lattice directions are another plausible explanation of this finding. Nevertheless, one has to be aware that the fwhm(Q_{xy}) of all peaks at $Q_z > 0$ Å^{-1} can be influenced by deviations of the water surface from the horizontal.

We find for myristic acid a tilt azimuth dispersed by about 5° around 0°, which differs from a tilt azimuth that is locked in a direction between 0° and 30° assumed in the continuum theory dealing with stripe textures.[20] In some previous publications,[11b,21] it was concluded from the occurrence of stripe textures that the monolayer is in a chiral phase such as smectic L. Our results suggest, however, that the dispersion of the tilt azimuth in monolayers of fatty acids and their methyl esters is not characteristic of a special phase but occurs generally in the tilted phases of these layers to different degrees. Asymmetric (11), ($1\bar{1}$) peaks are not only observed for myristic acid but also for palmitic acid and, although smaller, for methyl palmitate as well (Table 3). Whereas continuous changes of the molecular orientation occur in palmitic acid layers, no such continuous changes of orientation are observed in methyl palmitate layers (or they are at least too small to appear in the images). It becomes evident that myristic acid, palmitic acid, and methyl palmitate layers differ only with respect to the degree of the dispersion of the tilt azimuth.

So far, the phase in which the stripe textures occur has not been identified. Thus far nothing has been known about the elastic constants (Frank constants) for the bending and splay rigidity. These constants have been assumed to be related to the positional correlation lengths parallel and perpendicular to the tilt azimuth.[11b] Only the values of stearic acid,[2] which shows no stripe texture at all, have been available for estimating the Frank constants. The differences in the positional correlation length calculated from the different peaks (less than a factor of 2) can be used to estimate the ratio of Frank constants for myristic and palmitic acid. However, future experiments should be designed that avoid the influence from deviations of the water surface from the normal.

Conclusions

For the first time structural data for monolayers of fatty acids and their methyl and ethyl esters have been obtained under conditions where the typical textures are observed. In all monolayers studied here, the cross-sectional areas of the alkyl chains are about 20 Å^2, typical of the free rotator phases of *n*-alkanes. The highest cross-sectional area was observed for myristic acid, i.e., the substance with the shortest chain. The positional correlation lengths are between 100 and 200 Å. The monolayers of fatty acids differ from those of their methyl and ethyl esters especially by the higher polar tilt angles. At low surface pressures the fatty acid layers are in a phase with NN-tilted chains. For palmitic acid a transition to NNN-tilted chains can be observed. In methyl palmitate layers only a phase with NN-tilted chains occurs at 22 °C, whereas the chains are exclusively NNN-tilted in ethyl palmitate layers.

The occurrence of stripe textures in myristic acid monolayers coincides with the observation of a rectangular lattice with an asymmetric (11), ($1\bar{1}$) peak, which indicates a dispersion of the tilt azimuth with respect to the lattice directions at both 5 and 15 mN/m. The diffraction patterns suggest that the tilt azimuth is dispersed by about 5° around an NN direction at both surface pressures. This shows that the degree of the dispersion of the tilt azimuth is not directly correlated with the extent of the continuous change of orientation in the micrometer range (corresponding to the width of the stripes). The tilt azimuth is not locked to an angle between 0° and 30° as assumed in previous publications. The tilt azimuth also disperses in monolayers of palmitic acid and methyl palmitate with respect to the lattice directions; only the degree of the dispersion is different. The dispersion of the tilt azimuth is obviously not characteristic of a special monolayer phase.

Acknowledgment. Financial assistance from the Deutsche Forschungsgemeinschaft and the Fonds der Chemischen Industrie is gratefully acknowledged. We also thank K. Kjaer for help with setting up the X-ray experiment.

References and Notes

(1) (a) Overbeck, G. A.; Hönig, D.; Möbius, D. *Langmuir* **1993**, *9*, 555−560. (b) Overbeck, G. A.; Möbius, D. *J. Phys. Chem.* **1993**, *97*, 7999−8004.

(2) Kenn, R. M.; Böhm, C.; Bibo, A. M.; Peterson, I. R.; Möhwald, H.; Als-Nielsen, J.; Kjaer, K. *J. Phys. Chem.* **1991**, *95*, 2092−2097.

(3) (a) Dutta, P. *Phase Transitions Surf. Films 2, 1991*, **1991**, 183−200. (b) Shih, M. C.; Bohanon, T. M.; Mikrut, J. M.; Zschack, P.; Dutta, P. *Phys. Rev. A* **1992**, *45*, 5734−5737.

(4) (a) Peterson, I. R.; Brzesinski, V.; Kenn, R. M; Steitz, R. *Langmuir* **1992**, *8*, 2995−3002. (b) Peterson, I. R.; Kenn, R. M. *Langmuir* **1994**, *10*, 4645−4650.

(5) Kaganer, V. M.; Peterson, I. R.; Kenn, R. M.; Shih, M. C.; Durbin, M.; Dutta, P. *J. Chem. Phys.* **1995**, *102*, 9412−9422.

(6) (a) Foster, W. J.; Shih, M. C.; Pershan, P. S. *Mater. Res. Soc. Symp. Proc.* **1995**, *375*, 187−192. (b) Foster, W. J.; Shih, M. C.; Pershan, P. S. *J. Chem. Phys.* **1996**, *105*, 3307−3315.

(7) (a) Fischer, B.; Tsao, W.-M.; Ruiz-Garcia, J.; Fischer, Th. M.; Schwartz, D. K.; Knobler, C. M. *Thin Solid Films* **1996**, *284/285*, 110−114. (b) Fischer, B.; Tsao, M.-W.; Ruiz-Garcia, J.; Fischer, T. M.; Schwartz, D. K.; Knobler, C. M. *J. Phys. Chem.* **1994**, *98*, 7430−7435.

(8) Brezesinski, G.; Scalas, E.; Struth, B.; Möhwald, H.; Bringezu, F.; Gehlert, U.; Weidemann, G.; Vollhardt, D. *J. Phys. Chem.* **1995**, *99*, 8758−8762.

(9) (a) Gehlert, U.; Weidemann, G.; Vollhardt, D. *J. Colloid Interface Sci.* **1995**, *174*, 392−399. (b) Weidemann, G.; Gehlert, U.; Vollhardt, D. *Langmuir* **1995**, *11*, 864−871.

(10) Weidemann, G.; Vollhardt, D. *Langmuir* **1996**, *12*, 5114−5119.

(11) (a) Schwartz, D. K.; Ruiz-Garcia, J.; Qiu, X.; Selinger, J. V.; Knobler, C. M. *Physica A* **1994**, *204*, 606−615. (b) Ruiz-Garcia, J.; Qiu, X.; Tsao, M.-W.; Marshall, G.; Knobler, C. M.; Overbeck, G. A.; Möbius, D. *J. Phys. Chem.* **1993**, *97*, 6955−6957. (c) Qiu, X.; Ruiz-Garcia, J.; Knobler, C. M. *Mater. Res. Soc. Symp. Proc.* **1992**, *237*, 263−270.

(12) (a) Schwartz, D. K.; Tsao, M.-W.; Knobler, C. M. *J. Chem. Phys.* **1994**, *101*, 8258−8261. (b) Riviére, S.; Meunier, J. *Phys. Rev. Lett.* **1995**, *74*, 2495−2498.

(13) Qiu, X.; Ruiz-Garcia, J.; Stine, K. J.; Knobler, C. M.; Selinger, J. V. *Phys. Rev. Lett.* **1991**, *67*, 703−706.

(14) Fischer, T. M.; Bruinsma, R. F.; Knobler, C. M. *Phys. Rev. E* **1994**, *50*, 413−428.

(15) Overbeck, G. A.; Hönig, D.; Möbius, D. *Thin Solid Films* **1994**, *224*, 213−219.

(16) Dierker, S. B.; Pindak, R.; Meyer, R. B. *Phys. Rev. Lett.* **1986**, *56*, 1819−1822.

(17) (a) Als-Nielsen, J.; Möhwald, H. In *Handbook on Synchrotron Radiation*; Ebashi, S., Koch, M., Rubenstein, E., Eds.; Amsterdam: Oxford, New York, Tokyo, 1994; Vol. 4, pp 1−53. (b) Kjaer, K. Experimental Stations at HASYLAB, January 1994; pp 88−89. (c) Als-Nielsen, J.; Jacquemain, D.; Kjaer, K.; Lahav, M.; Leiveiller, F.; Leiserowitz, L. *Phys. Rep.* **1994**, *246*, 251−321.

(18) Weidemann, G.; et al., *Langmuir*, submitted.

(19) Howes, P. B.; Kjaer, K. Annual Report 1996; Hamburger Synchrotronstrahlungslabor HASYLAB am Deutschen Elektronensynchrotron DESY, 1996; p 445.

(20) Selinger, J. V.; Wang, Z.-G.; Bruinsma, R. F.; Knobler, C. M. *Phys. Rev. Lett.* **1993**, *70*, 1139−1142.

(21) Riviere, S.; Henon, S.; Meunier, J. *Phys. Rev. E* **1994**, *49*, 1375−1382.